NASA TECHNICAL NOTE

NASA TN D-7073

NASA TN D-7073

FRETTING OF SECONDARY-SEAL-RING CANDIDATE MATERIALS IN AIR AT TEMPERATURES TO 816° C

by Robert C. Bill

Lewis Research Center
and
U.S. Army Air Mobility R&D Laboratory
Cleveland, Ohio 44135

NATIONAL AERONAUTICS AND SPACE ADMINISTRATION • WASHINGTON, D. C. • NOVEMBER 1972

1. Report No.	2. Government Accession No.	3. Recipient's Catalog No.
NASA TN D-7073		

4. Title and Subtitle	5. Report Date
FRETTING OF SECONDARY-SEAL-RING CANDIDATE MATERIALS IN AIR AT TEMPERATURES TO 816° C	November 1972
	6. Performing Organization Code
7. Author(s)	8. Performing Organization Report No.
Robert C. Bill	E-7025
	10. Work Unit No.
9. Performing Organization Name and Address	501-24
NASA Lewis Research Center and U.S. Army Air Mobility R&D Laboratory Cleveland, Ohio 44135	11. Contract or Grant No.
	13. Type of Report and Period Covered
12. Sponsoring Agency Name and Address	Technical Note
National Aeronautics and Space Administration Washington, D.C. 20546	14. Sponsoring Agency Code

15. Supplementary Notes

16. Abstract

Superalloys containing chromium showed decreasing fretting damage with increasing temperature to 816° C. This trend was related to the ability of the alloys to generate self-protecting oxide films. The damage at 816° C was one-third to one-tenth of that at 23° C. Osmium, chromium, and chromium carbide platings were fretted at 23° and 450° C. Osmium was extremely protective at 23° C but oxidized excessively at 450° C. Chromium and chromium carbide gave about the same protection at 450° C as the oxide films that formed on the superalloys. High-graphite and low-graphite carbons were fretted at 23° and 327° C. High-graphite carbon was superior at 327° C, but low-graphite carbon was the best material examined at 23° C.

17. Key Words (Suggested by Author(s))

Fretting
Oxidation
Oxide films
Fatigue-corrosion
Graphite
Superalloys

18. Distribution Statement

Unclassified - unlimited

19. Security Classif. (of this report)	20. Security Classif. (of this page)	21. No. of Pages	22. Price*
Unclassified	Unclassified	28	$3.00

* For sale by the National Technical Information Service, Springfield, Virginia 22151

FRETTING OF SECONDARY-SEAL-RING CANDIDATE MATERIALS IN AIR AT TEMPERATURES TO 816° C

by Robert C. Bill

Lewis Research Center and
U. S. Army Air Mobility R&D Laboratory

SUMMARY

Fretting experiments were conducted on several alloys in like metal pairs at temperatures up to 816° C (1500° F). These alloys included René-41, Inconel X-750, Monel-400, TZM, 304 stainless steel, Haynes-25, and Haynes-188. Haynes-188 was the best of the alloys examined at elevated temperature, while TZM showed the least fretting damage of the alloys examined at room temperature. Scanning electron microscopy and X-ray dispersion analysis indicated that the fretting scar regions of the chromium containing alloys were richer in chromium than the surrounding unfretted surface. The surface chromium was undoubtedly present as an oxide, probably Cr_2O_3, a hard protective film. Fretting at elevated temperatures was due largely to abrasion of the protective oxide films and to a fatigue-corrosion mechanism that aided in surface disruption.

Electroplated osmium, chromium, and bonded chromium carbide coatings were examined at 23° C (74° F) (room temperature) and 450° C (840° F). Osmium was extremely effective in resisting fretting at room temperature but oxidized excessively at 450° C (840° F) with a large amount of fretting damage. The oxide formed on chromium plating gave about the same protection at 450° C (840° F) as the naturally occurring oxide films on the alloys containing chromium.

Low- and high-graphite carbon specimens were fretted against themselves, against three ceramic materials (boron nitride, silicon carbide, and aluminum oxide) and against five metals (304 stainless steel, Inconel X-750, Haynes-25, TZM, and 99.9 percent nickel). Experiments were conducted at 23° and 327° C (74° and 620° F). It was found that the high-graphite carbon showed less fretting wear at 327° C (620° F) than at room temperature and was far superior to the low-graphite carbon at 327° C (620° F). Except for osmium-coated 304 stainless steel, the low-graphite carbon was the best material examined at room temperature but underwent severe fretting damage at 327° C (620° F).

INTRODUCTION

Fretting wear characterized by low-amplitude vibratory sliding between mating parts is a problem in many structural and engine components of aircraft. Typical examples include structural fasteners, control surface support bearings, airframe hinges, and turbine and compressor blade roots. A particular area of concern in this investigation is the engine main-shaft seal assembly.

In the turbine section of a jet aircraft engine, the main-shaft face seal is used to separate the 650° C (1200° F) turbine gases from the bearing compartment which contains oil at 200° C (400° F). There are two leakage paths in the face-seal assembly. One is through the gap between the seal nosepiece and the rotating seat; the other is between the secondary seal ring (piston-ring type) and the carrier. The secondary seal ring is not exposed to the high sliding speeds of the face-seal nosepiece. However, because of unavoidable runout, the secondary seal ring is subjected to a vibratory axial motion relative to the carrier. This vibratory motion results in fretting damage to the secondary seal, which causes nearly half of the total seal leakage to pass through the secondary seal (ref. 1).

The mechanisms of fretting have been investigated (refs. 2 to 5), and there is agreement that damage is initiated by adhesive forces acting between the contacting surfaces. In metals, the latter stages of fretting are characterized by corrosion and subsurface fatigue with a possible interaction between these two (refs. 3 to 5).

Various high-temperature alloys including Inconel X-750 and 304 stainless steel have been used as secondary seal materials. TZM (a molybdenum-base alloy), Haynes-25, and a high-temperature carbon have also been used on an experimental basis (ref. 1).

The purpose of this report is to study fretting by testing a wide range of materials as possible candidates for the secondary-seal problem area. Based on a thermal analysis of the face-seal design (ref. 1), the actual service temperature of the secondary seal is about 320° C (600° F). The candidate materials must retain strength and resist oxidation up to this temperature. Ease of fabrication and low-to-moderate elastic modulus to allow for handling and assembly without fracture are desirable features. The materials studied included seven high-temperature alloys, three experimental protective coatings on 304 stainless steel, and three different types of carbon. All of the materials examined are listed in table I with a brief description of each. The alloys were fretted in like metal pairs at the following temperatures: 23° C (74° F) (room temperature) and 216°, 327°, 450°, 540°, and 816° C (420°, 620°, 840°, 1000°, and 1500° F). This extended temperature range for the alloys provided data applicable to other high-temperature uses of these materials. The coated specimens in like metal pair combinations were fretted at 23° and 450° C (74° and 840° F). The carbon materials were

fretted against four alloys and three ceramic materials at 23° and 327° C (74° and 620° F).

The basis for comparison of results included calculated fretting wear volumes, photomicrographs, scanning electron microscope (SEM) micrographs, elemental analysis by X-ray dispersion, and observations of gross specimen change (e.g., catastrophic oxidation at elevated temperatures).

APPARATUS

A schematic diagram of the fretting rig is shown in figure 1, and a detailed description of its operation is included in reference 2. In essence, a linear oscillatory motion is provided by an electromagnetically driven vibrator with the frequency controlled by a variable oscillator. The load is applied to the specimen by placing precision weights in a load pan which is hung from the load arm.

The fretting specimens consist of a stationary, spherical-tip 4.75-millimeter-(3/16-in.-) radius upper specimen in contact with a flat lower specimen which is driven by the vibrator.

During high-temperature experiments, the specimens and grip assemblies were surrounded by a 310 stainless steel susceptor which was heated by an induction coil. The specimen temperature was monitored by a thermocouple probe. The grips when tightened stored elastic energy and assured that no specimen slippage would occur as a result of differential thermal expansion.

PROCEDURE

The procedure for conducting room-temperature experiments is described in detail in reference 2. In the present investigation, room air was at $23^{\circ}\pm1^{\circ}$ C ($74^{\circ}\pm2^{\circ}$ F), and the relative humidity was 35±10 percent. The normal load between the two specimens was 1.47 newtons. The frequency of the oscillations was controlled at 80.0±0.2 hertz. The peak-to-peak amplitude was 75×10^{-6} meter (0.003 in.). A typical experiment was 2.9×10^{5} cycles in duration and required 1 hour of fretting time.

Specimen temperature was controlled by setting the plate current of the induction power supply to such a level that the specimen temperature stabilized at the desired temperature. The alloys were examined in like metal fretting pairs at six different temperatures: 23°, 216°, 327°, 450°, 540°, and 816° C (74°, 420°, 620°, 840°, 1000°, and 1500° F). The 304 stainless steel specimens with applied protective coatings were fretted in like material combinations at 23° and 450° C (74° and 840° F); the carbon

specimens (used as the flat, lower specimen) were fretted at 23° and 327° C (74° and 620° F) against a variety of alloys and ceramic materials. The actual temperatures remained within 5.5° C (10° F) of the desired temperatures.

Before fretting, the flat specimen was lapped to a matte finish. All specimens were scrubbed with levigated alumina and rinsed in distilled water. After this treatment, a surface profilometer was used to measure the surface roughness on the metal and carbon specimens at about 0.25 and 0.90 micrometer (10 and 35 μin.) (centerline average), respectively.

Following each experiment, the specimens were removed from the rig and a photomicrograph was made of the fretting scar on both the flat surface and the spherical surface. Next a light section microscope was used to measure the volume of material removed from the fretting scar on the flat specimens. For the metal specimens fretted at room temperature, it was necessary to remove the debris ultrasonically to get accurate wear scar measurements. In every other case, however, the damage scar was left untouched.

The specimens that were examined in the SEM either were alloys fretted at elevated temperatures or were carbon materials (except for the osmium-coated specimen). In all of these cases, the small quantity of debris did not interfere with the SEM observations. Therefore, no ultrasonic cleaning procedures were required prior to SEM examination.

MATERIALS

The alloys fretted in like metal pairs were Inconel X-750, René-41, Monel-400, 304 stainless steel, TZM, Haynes-25, and Haynes-188. The nominal compositions, room-temperature hardnesses, and initial heat treatments of these metals are listed in table I.

A 2.5-micrometer (0.1-mil) electrodeposited osmium plating, a 10-micrometer (about 0.4-mil) electrodeposited chromium plating, and a 10-micrometer (about 0.4-mil) bonded chromium carbide coating were investigated as possible antifretting coatings These platings were all deposited on 304 stainless steel and were subjected to fretting in like material combinations.

Three different carbons were studied in this investigation (see table I): a high-purity high-graphite carbon with no added oxidation inhibitors and two low-graphite seal grade carbon materials, one containing a high-temperature oxidation inhibitor and the other containing no inhibitor. The oxidation inhibitor is believed to be a mixture of zinc phosphate and boron phosphate, but the exact composition is unknown.

With the exception of one experiment involving 99.9 percent nickel, the carbon specimens were used as the lower, flat specimen. The materials against which the carbons were fretted (composing the upper, spherical specimens) included three ceramic materials (silicon carbide, boron nitride, and aluminum oxide) and five metals (304 stainless steel, Inconel X-750, Haynes-25, TZM, and 99.9 percent nickel). The nominal compositions and room-temperature hardnesses of the metals are shown in table I. The ceramic materials were of commercial purity (>99 percent), the aluminum oxide and boron nitride were hot pressed, and the silicon carbide was made by a vapor-deposition process.

RESULTS AND DISCUSSION

Fretting of Alloys

The results of the experiments conducted on the alloys are summarized in table II. All materials were subjected to 2.9×10^5 fretting cycles in like metal pair combinations.

The best overall material examined was the Haynes-188 alloy, which is generally acknowledged to be a good high-temperature oxidation-resistant alloy. In the temperature range at which the secondary seal operates, Haynes-188, TZM, and René-41 appeared to be the best choices among the alloys. The good performance of TZM up to 450° C (840° F), where bulk oxidation begins to occur may be due to the lubricating nature of the molybdenum oxide debris (ref. 2). The debris around the scars in figure 2 is believed to be molybdenum dioxide.

After being fretted at 816° C (1500° F), the damage scars on 304 stainless steel and Haynes-25 had a material buildup protruding 4 to 8 micrometers (0.16 to 0.32 mil) above the surface. This may be seen in figure 3, showing light section micrographs of the damage scars on 304 stainless steel and Inconel X-750 (for comparison) produced by fretting at 816° C (1500° F). In any close contacting device (e.g., airframe bearing), such buildup could lead to increased interfacial loading and higher frictional force, which would promote further damage.

A general trend observed in the alloys containing chromium as a major alloying element was that fretting wear decreases with increasing temperature. Haynes-25 shows a deviation from this trend at 216° C (420° F). Figure 4 shows a plot of the fretting wear against temperature for Haynes-188, René-41, and Inconel X-750, the three best performing alloys over the entire temperature range. Such a trend has also been reported for carbon steels fretted at temperatures up to 500° C (932° F) (ref. 6) and for several superalloy combinations at temperatures up to 260° C (500° F) (ref. 7).

This trend is best understood in terms of the oxide film that forms on the alloy surface. Virtually all metals in contact with air will be covered quickly with an oxide layer. This oxide layer grows in thickness by an ion-diffusion mechanism (ref. 8). The property that makes certain alloys especially oxidation resistant is the formation of oxide films that resist ion diffusion and thus render the oxidation process self-limiting. Such oxide films may be formed by the simple oxidation of the bulk metal, as in the case of aluminum, or they may result from the selective oxidation of one or more atomic species in an alloy system.

In the nickel-chromium system (pertaining to René-41 and Inconel X-750), high-temperature oxidation of alloys containing more than 10 percent chromium selectively forms chromium oxide (Cr_2O_3) on the alloy surface (ref. 8). Chromium oxide is a hard, tenacious film that affords protection to the alloy against further oxidation. In a fretting situation, the presence of this film may be expected to reduce adhesion between the mating parts and reduce fretting damage. There is evidence for this in figure 5, which shows a series of photographs taken of René-41 specimens.

SEM photographs (fig. 6), combined with an X-ray dispersion analysis (fig. 7), indicate the fretting mechanisms operating at 816° C (1500° F) on Inconel X-750. The dark regions of figure 6(a) correspond to the high areas where rubbing actually occurs; the dark shade indicates that the surface is highly oxidized. The smoothness of the general surface and the presence of scratches (figs. 6(b) and (c)) strongly suggest that the primary mechanism of surface disruption is abrasion caused by hard, broken Cr_2O_3 coated particles. The lower areas (areas at a level below the contacting surface) filled with loose oxidized debris (the brightly glowing particles) cover about one-third of the scar area in figure 6(a). Figure 6(d), a high magnification micrograph of the edge between a high area and a low area, shows a layered structure with the loose debris being generated at these edges.

The area shown in figure 6(d) was subjected to an X-ray dispersion analysis and compared with a similar analysis taken at a spot away from the fretting scar. The results are shown in figure 7. The important point to note is that in the fretting scar (fig. 7(a)), the chromium peak is about 80 percent as high as the primary nickel peak, while outside the scar (fig. 7(b)), the primary chromium peak is less than half the height of the primary nickel peak. This indicates that there is a significantly higher chromium concentration in the fretting scar than in the surrounding surface areas.

Considering that the characteristic X-rays originate from several micrometers beneath the specimen surface (ref. 9), the higher chromium peak in the fretting scar must indicate subsurface distressing of the alloy due to the fretting action. If selective surface oxidation alone accounted for the chromium concentration near the surface of the fretting scar, there should be little difference between the X-ray measurements of figures 7(a) and (b). There are two explanations that could account for the X-ray dispersion results:

(1) Plastic deformation of the surface layers in the fretting scar resulted in increased dislocation density and consequently the diffusion of more chromium to the surface.

(2) The surface in the fretting scar was undermined with fatigue cracks with chromium selectively oxidized at the crack surfaces giving rise to the detection of more chromium in the scar.

While the first hypothesis cannot be entirely rejected, the second can adequately explain the SEM photographs of figure 6 as well as the lower overall X-ray intensity of figure 7(a) compared to 7(b). The layer structure shown in figure 6(d) resulted from the intersection of fatigue cracks with the surface. The lower overall X-ray intensity is due to the formation of more oxide on the crack surfaces of the fretting scar producing a lower average atomic number. The propagation of these cracks is aided by oxidation and results in debris generation and surface disruption. Such a mechanism has been identified in titanium fretted at room temperature (ref. 2).

Fretting of Osmium, Chromium, and Chromium Carbide Coatings

After 2.9×10^5 fretting cycles at room temperature and 450° C (840° F) in like material pair combinations, the wear volume was measured (fig. 8). Photomicrographs of the fretting scars are shown in figure 9. At room temperature the osmium coating was superior since no coating penetration was observed. However, red debris (indicating coating penetration) was present at room temperature for the chromium and chrome carbide coatings. At 450° C (840° F), however, the osmium coating was penetrated by oxidation damage which resulted in the formation of a deep scar on the underlying 304 stainless steel. The chromium coating afforded adequate protection to the substrate material and the result was somewhat less wear volume than for the unprotected 304 stainless steel. The performance of the chromium carbide coating at 450° C (840° F) was difficult to assess because of black, compacted debris concentrated in the center of the wear scar. The damage volume measured is an estimate based on the maximum depth of a pit observed in the scar center. From the appearance of the damage scar, chromium carbide was not as effective as chromium, the best coating examined at 450° C (840° F).

An SEM examination was made of the osmium coating after being exposed to 10^3, 10^4, and 3×10^5 fretting cycles at room temperature. The results are shown in figure 10. A network of cracks divides the electroplated coating into small platelets 3 or 4 micrometers in diameter. In figure 10(b), some platelets are missing even where no fretting has occurred. In view of the imperfections present, it is remarkable that after 3×10^5 fretting cycles only limited coating penetration has occurred in the center of the contact region (fig. 10(d)). It could well have been that the crack network served as a trap for

abrasive wear particles. This may explain why the cracks are so obscure in the contact region.

Fretting of Carbons at Room Temperature and 326° C

It was found that the high-graphite carbon flats, when fretted against 304 stainless steel, Inconel X-750, and Haynes-25 showed significantly less damage at 327° C (620° F) than at room temperature (fig. 11). Comparison of figure 11 with data in table II shows that, when fretted against the alloys at 327° C (620° F), the high-graphite carbon generally underwent three to five times as much damage as the alloys did when fretted against themselves in the metal pairs. The trend of decreasing damage with increasing temperature was also observed when the high-graphite carbon was fretted against silicon carbide and aluminum oxide. Boron nitride was the exception in that far more damage on the high-graphite flat was observed after fretting at 327° C (620° F) than at room temperature. Part of the reason for this may be the reaction of boron nitride to form boric oxide or boron carbide, both abrasive materials under some conditions. Figure 12 shows the presence of debris around the fretting scar (high-graphite flat fretted against boron nitride). The extent of damage may be appreciated by comparison of figure 12 with figure 13, which shows the scar produced by fretting high-graphite carbon against aluminum oxide.

The presence of the oxidation inhibitor in the low-graphite carbon did not have a significant effect on the fretting results at either room temperature or 327° C (620° F). In contrast to the high-graphite carbon, the low-graphite carbon underwent more fretting damage at 327° C (620° F) than at room temperature (fig. 14). This trend was particularly marked when the carbon was fretted against the metal alloys. Comparison of figure 14 with figure 8 and the data in table II reveals that, except for osmium plated 304 stainless steel, low-graphite carbon is the best material examined at room temperature.

An SEM study indicated no qualitative differences between the fretting scars on the low-graphite carbon and the high-graphite carbon after being fretted against the metal alloys. Figure 15 (low-graphite carbon fretted against Inconel X-750) shows evidence of some abrasive and surface shearing action. Note, however, that very little debris has accumulated around the fretting scar.

In order to see the results of fretting the carbons against a softer metal, high-graphite carbon and low-graphite carbon flats were fretted against a hemispherical-tip nickel rider of 99.9 percent purity at room temperature. The damage scar volumes on the carbon flats were 100×10^{-5} and 22×10^{-5} cubic millimeter for the high and low graphite, respectively. Figure 16 shows a peculiar transfer deposit of nickel on the graphite

surface. Physical appearance and the X-ray dispersion analysis shown in figure 16(c) identified the deposit as metallic nickel combined with graphitic debris.

The metallic deposits formed on the graphite were partly a consequence of the contact geometry. No such deposit was seen when the geometry was reversed, that is, when a spherical graphite specimen was fretted against a nickel flat. Possibly the distribution of stresses at the edges of the contact region in the spherical metallic surface led to a cyclic extrusion type of process. Figure 17 shows a two-dimensional approximation of the stress state of elements near the edge of the contact region of the spherical specimen and the flat specimen. The stress component σ_{yy} is approximately given by

$$\sigma_{yy} = \frac{L}{A}$$

where L is the contact load and A is the area of the damage scar. Material constraints result in the σ_{xx} term. In the flat specimen, σ_{xx} is given by

$$\sigma_{xx} = \nu\sigma_{yy}$$

where ν is the Poisson ratio. Because of the spherical geometry, the absolute value of σ_{xx} is smaller in the spherical specimen than in the flat specimen and is assumed to be zero in figure 17. The surface shear stress is simply given by

$$\tau_f = \mu\sigma_{yy}$$

where μ is the local coefficient of friction. The large hydrostatic stress component of the flat geometry makes plastic yielding of the element on the flat specimen difficult. The nearly uniaxial compressive loading in the spherical geometry enables the material to yield more readily under the action of the cyclic frictional shearing. The Mohr's circle representations of the stress states summarize this. For a given normal load and frictional shear stress, higher maximum shear stresses are reached in the spherical bullet than in the flat.

A surprising difference was observed in the nickel debris generated on the low-graphite carbon (fig. 18). The carbon surface showed evidence of abrasive damage. The debris was in the form of fine particles loosely scattered outside the fretting scar at diametrically opposite ends of the scar that lie on an axis parallel to the direction of the fretting motion. Such particles may be seen in figure 18(c). The glow of the particles and the X-ray dispersion analysis (fig. 18(d)) indicate that they are nickel oxide particles.

CONCLUSIONS

Based on the results of this investigatigation, the following conclusions may be drawn concerning the selection of a suitable secondary-seal material from the standpoint of resisting fretting at various temperatures up to 816° C (1500° F):

1. The high-chromium-content alloys showed the greatest potential of the materials investigated. Haynes-188 proved to be the best.

2. When compared to other high-chromium alloys, TZM showed good resistance to fretting up to temperatures of 450° C (840° F), where severe oxidation began to occur.

3. The most effective plating examined at 450° C (840° F) was chromium; however, the effectiveness of chromium was not significantly better than that of the oxide films that formed on the high-chromium alloys.

4. High-graphite carbon was superior to the low-graphite carbon at the secondary-seal operating temperature (327° C; 620° F). However, the fretting damage of the high-graphite carbon when fretted against the superalloys was generally three to five times greater than the damage measured on the alloys when they were fretted against themselves.

The following general statements may be made regarding fretting in the materials studied in this investigation:

1. Superalloys that formed a protective chromium oxide film generally showed decreasing fretting damage with increasing temperature up to 816° C (1500° F). The dominant fretting mechanism in superalloys at elevated temperature was abrasion with a fatigue-corrosion mechanism aiding surface disruption.

2. Electroplated osmium was extremely effective in reducing fretting damage at room temperature but rapidly oxidized at 450° C (840° F).

3. Except when fretted against boron nitride and TZM, high-graphite carbon showed less fretting damage at 327° C (620° F) than at room temperature and was superior to low-graphite carbon at 327° C (620° F). Low-graphite carbon, the best uncoated material at room temperature, showed more fretting damage at 327° C (620° F) than at room temperature. Surface shearing and abrasion were the dominant fretting mechanisms operating in the carbons.

Lewis Research Center,
National Aeronautics and Space Administration,
and
U.S. Army Air Mobility R&D Laboratory,
Cleveland, Ohio, August 2, 1972,
501-24.

REFERENCES

1. Povinelli, V. P.; and McKibben, A. H.: Development of Mainshaft Seals for Advanced Air Breathing Propulsion Systems - Phase III. Rep. PWA-4263, Pratt & Whitney Aircraft (NASA CR-72987), July 25, 1971, p. 35.

2. Bill, Robert C.: Fretting Wear in Titanium, Monel-400, and Cobalt 2.5-Percent Molybdenum Using Scanning Electron Microscopy. NASA TN D-6660, 1972.

3. Godfrey, D.; and Bisson, E. E.: NACA Studies of Mechanism of Fretting (Fretting Corrosion) and Principles of Mitigation. Lubr. Eng., vol. 8, no. 5, Oct. 1952, pp. 241-243, 262-263.

4. Hurricks, P. L.: The Mechanism of Fretting - A Review. Wear, vol. 15, 1970, pp. 389-409.

5. Bethune, B.; and Waterhouse, R. B.: Adhesion of Metal Surfaces Under Fretting Conditions. I. Like Metals in Contact. Wear, vol. 12, 1968, pp. 289-296.

6. Hurricks, P. L.; and Ashford, K. S.: The Effect of Temperature on the Fretting Wear of Mild Steel. Proc. Inst. Mech. Eng., vol. 184, pt. 3L, 1969-70, p. 165.

7. Swikert, Max A.; and Johnson, Robert L.: Friction and Wear Under Fretting Conditions of Materials for Use as Wire Friction Dampers of Compressor Blade Vibration. NASA TN D-4630, 1968.

8. Kofstad, Per: High-Temperature Oxidation of Metals. John Wiley & Sons, Inc., 1966, p. 272.

9. Barrett, Charles S.: Structure of Metals, Crystallographic Methods, Principles, and Data. Second ed., McGraw-Hill Book Co., Inc., 1952, p. 56.

TABLE I. - MATERIAL COMPOSITIONS AND DESCRIPTIONS

(a) Superalloys

Alloy	Nickel	Cobalt	Iron	Chromium	Molybdenum	Tungsten	Titanium	Aluminum	Other constituents	Room temperature hardness	Thermomechanical history
	Nominal composition, wt. %										
René-41	Balance	11	-------	19	10	--	3	1.5	----------	Rockwell C 34	Solution treated; aged at 760° C (1400° F)
Inconel X-750	Balance	-------	7	15	-------	--	2.5	0.7	Columbium, ~1	Rockwell C 26	Solution treated
Monel-400	Balance	-------	2.5	--	-------	--	---	---	Copper, 29; manganese, ~2; carbon, 0.3; sulfur, 0.5	Rockwell B 56	Cold worked (solid solution alloy)
TZM	-------	-------	-------	--	Balance	--	0.5	---	Zirconium, ~0.08	Rockwell C 11	Annealed at 1370° C (2500° F)
304 stainless steel	10	-------	Balance	19	-------	--	---	---	Carbon, ~0.05	Rockwell C 19	Cold worked
Haynes-25	10	Balance	-------	20	-------	15	---	---	----------	Rockwell C 39	Solution treated; cold worked
Haynes-188	22	Balance	3	22	-------	14	---	---	Carbon, ~0,1; manganese, 1; lanthanum, 0.09	Rockwell C 12	Solution treated
Nickel	99.9	-------	-------	--	-------	--	---	---	----------	Rockwell B 80	Cold drawn rod

(b) Carbons

Carbon	Graphite, percent	Average grain size, μm	Nominal density, g/cm^3
Low-graphite carbon with oxidation inhibitor	~20	25	----
Low-graphite carbon without oxidation inhibitor	~20	25	1.75
High-graphite carbon	~90	150	1.6

TABLE II. - FRETTING SCAR VOLUMES OF VARIOUS ALLOYS

AT TEMPERATURES TO 820° C (1500° F)

Material	Temperature, °C (°F)					
	23 (74)	216 (420)	327 (620)	450 (840)	540 (1000)	820 (1500)
	Fretting scar volume, mm^3					
Inconel X-750	33×10^{-5}	20×10^{-5}	12×10^{-5}	8×10^{-5}	10×10^{-5}	12×10^{-5}
René-41	24	13	8	7	2	2
Monel-400	31	100	50	10	20	[a]15
TZM	14	16	3	[b]4	(c)	(c)
304-stainless steel	53	24	23	6.4	2	(d)
Haynes-188	31	7	3	2	7	2
Haynes-25	51	100	31	2	2	(d)

[a]Excessive scaling.

[b]Large amount of surface oxidation.

[c]Catastrophic oxidation.

[d]Buildup of oxidized material in fretting scar.

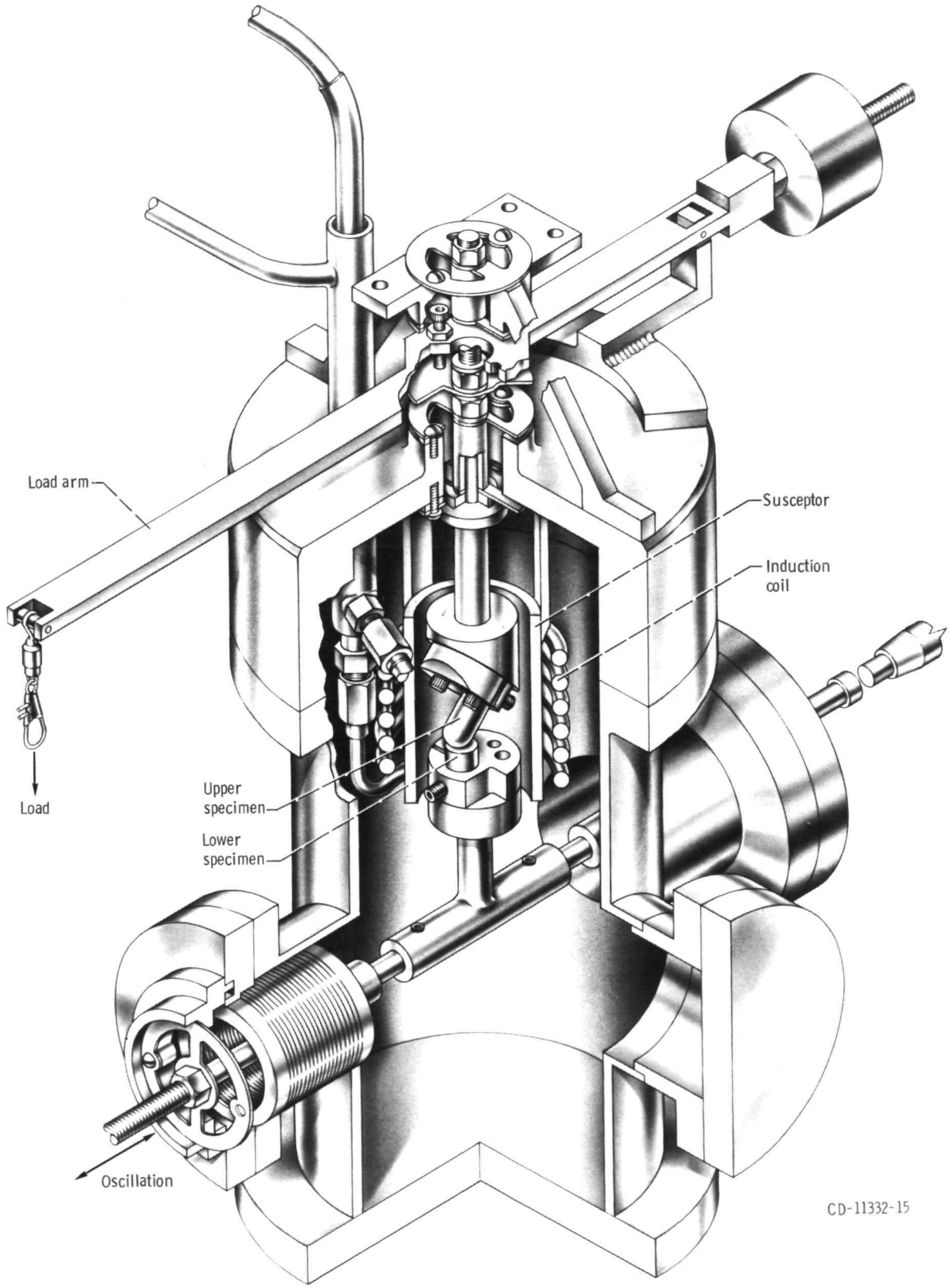

Figure 1. - Fretting apparatus.

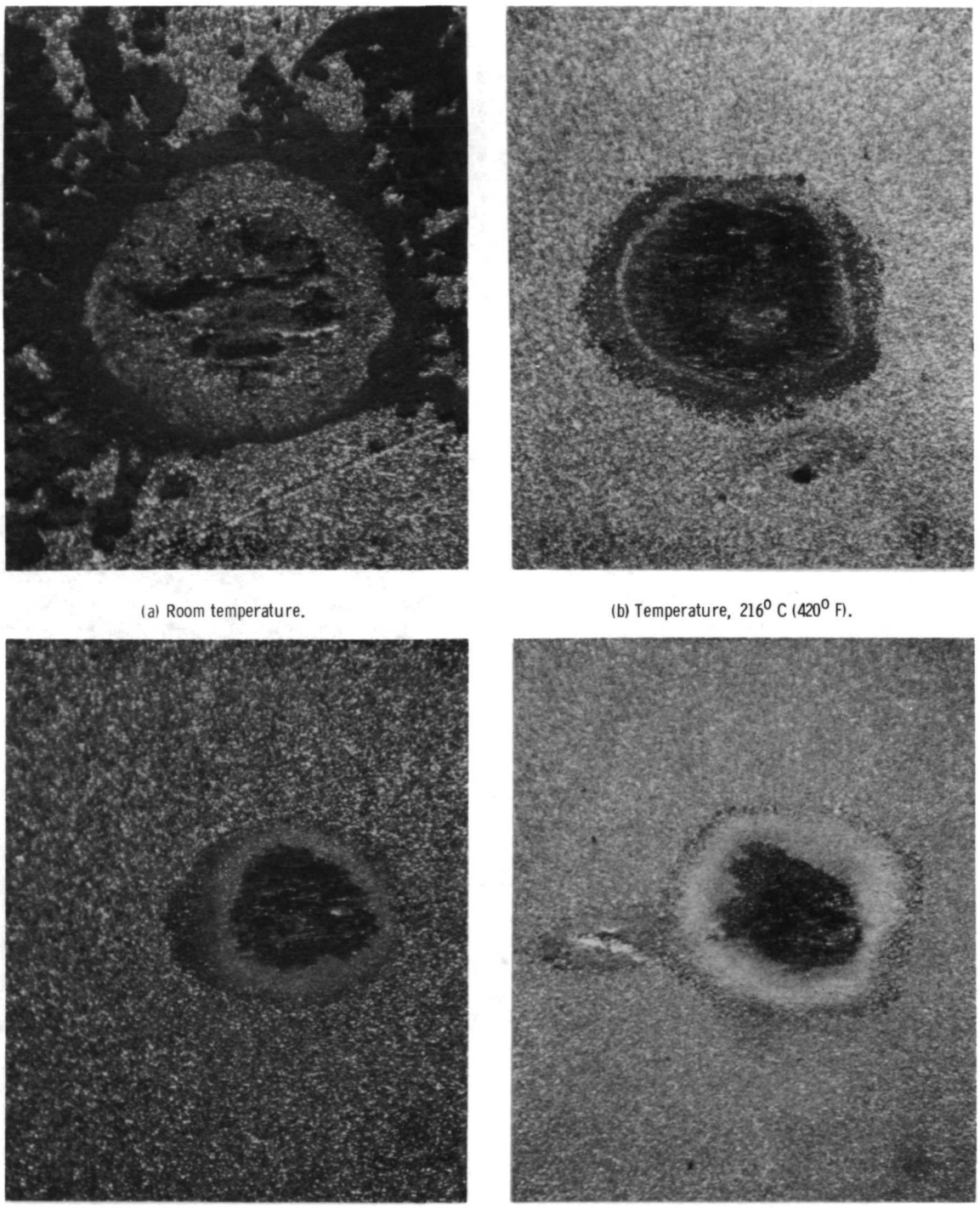

(a) Room temperature.

(b) Temperature, 216^{0} C (420^{0} F).

(c) Temperature, 327^{0} C (620^{0} F).

(d) Temperature, 450^{0} C (840^{0} F).

Figure 2. - TZM fretted against TZM. Frequency, 80 hertz; normal load, 1.47 newtons; number of cycles, 2.9×10^{5}; amplitude, 75×10^{-6} meter. X75.

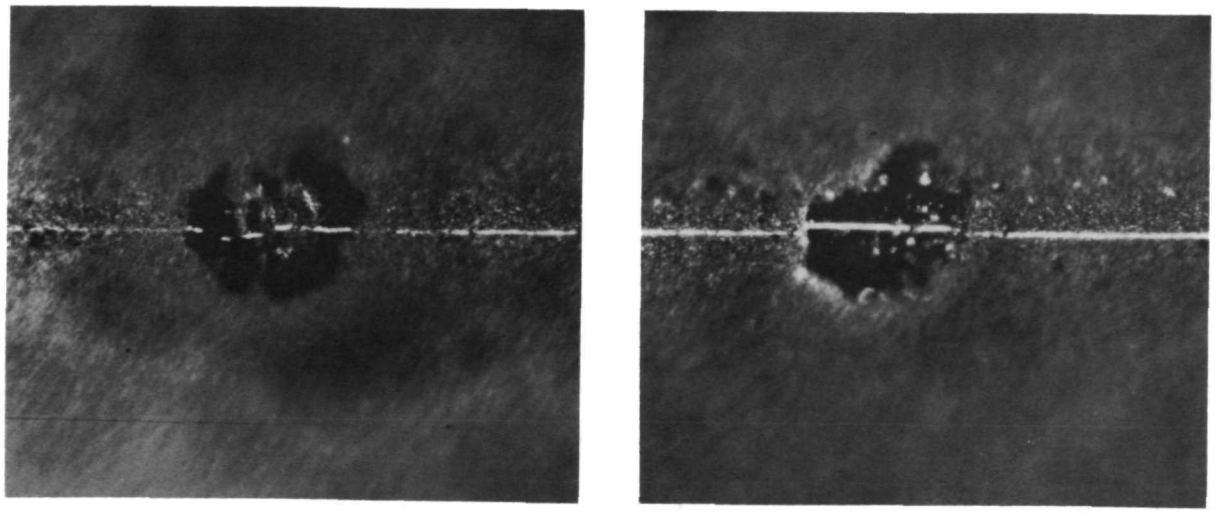

(a) Inconel X-750 fretted against Inconel X-750; note depression in fretting scar.

(b) 304 stainless steel fretted against 304 stainless steel; note scar elevated above surrounding surface.

Figure 3. - Light section micrographs of fretting scars produced on Inconel X-750 and 304 stainless steel. Frequency, 80 hertz; normal load, 1.47 newtons; number of cycles, 2.9×10^5; amplitude, 75×10^{-6} meter; temperature, 816^0 C (1500^0 F); X135 in relief; X95 in image plane.

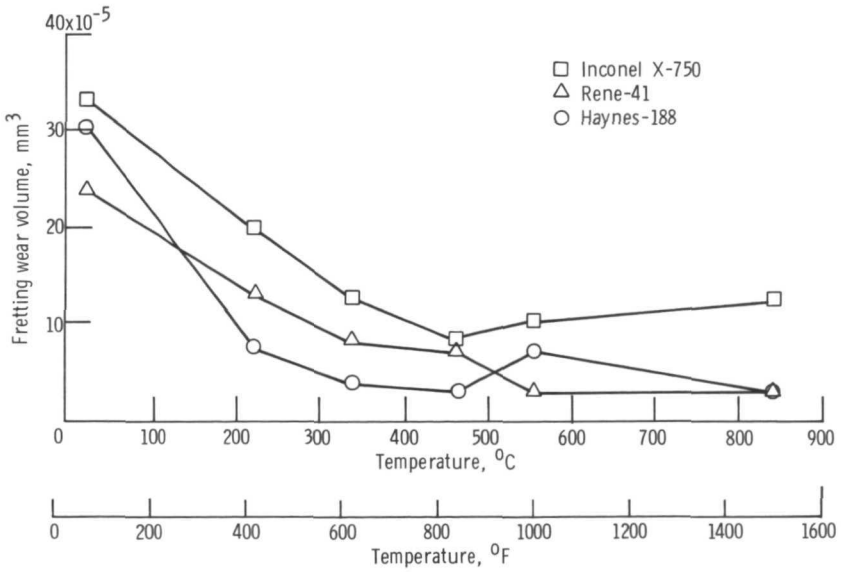

Figure 4. - Fretting wear volume as function of temperature for Inconel X-750, Rene-41, and Haynes-188. Frequency, 80 hertz; normal load, 1.47 newtons; number of cycles, 2.9×10^5; amplitude, 75×10^{-6} meter.

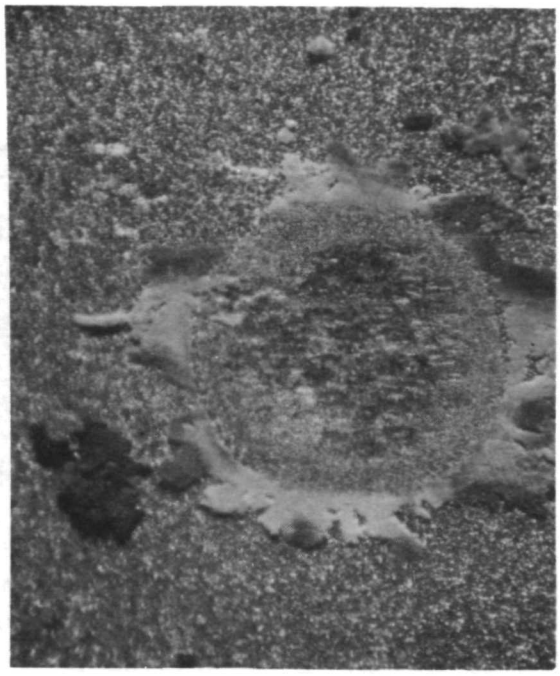

(a) Room temperature.

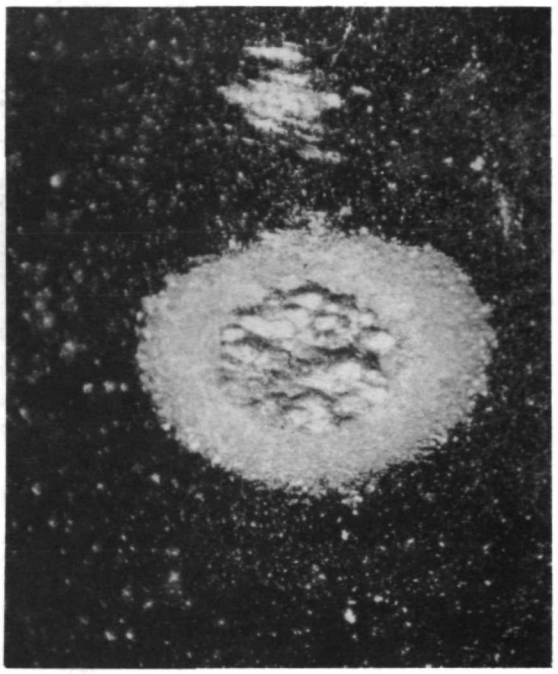

(b) Temperature, 450° C (840° F).

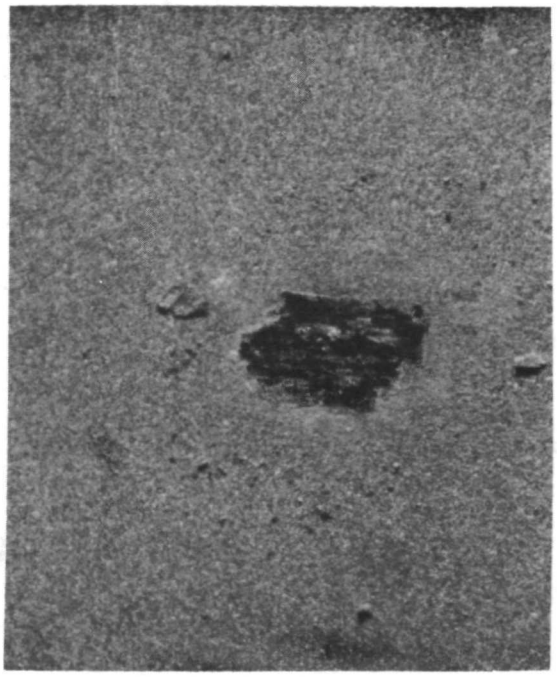

(c) Temperature, 820° C (1500° F).

Figure 5. - René-41 fretted against René-41. Frequency, 80 hertz; normal load, 1.47 newtons; number of cycles, 2.9×10^5. X75.

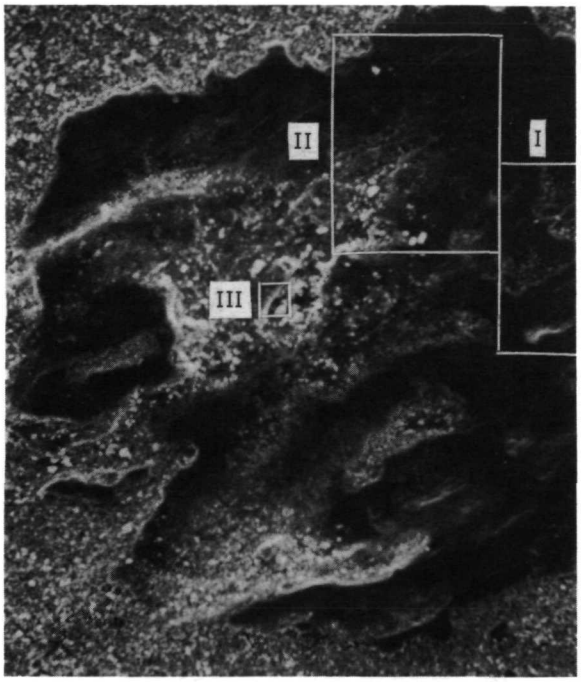

(a) Overview. X300.

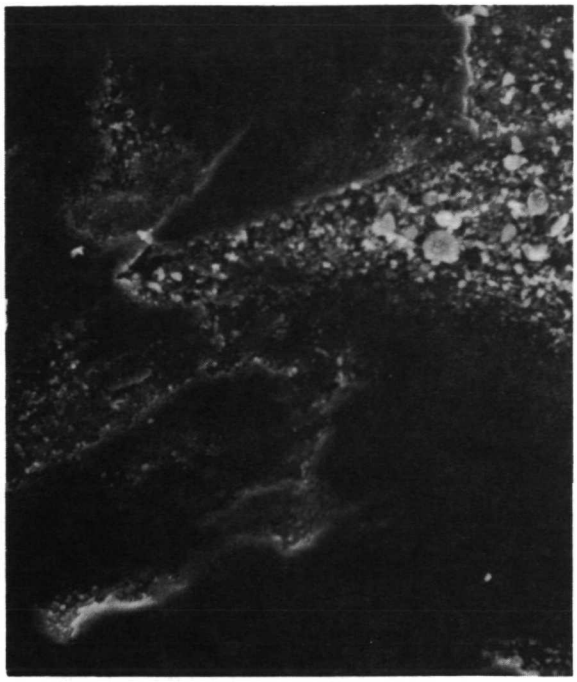

(b) Upper right of overview, area I. X900.

(c) Upper center of overview showing apparent surface scratches, area II. X900.

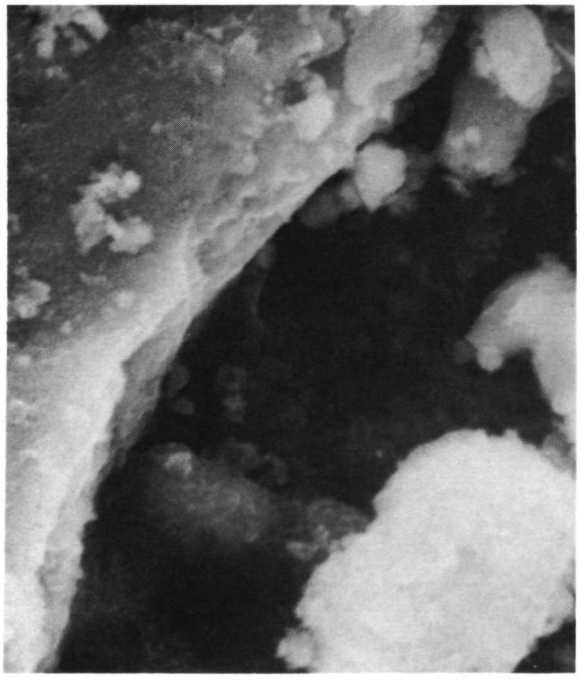

(d) Central region of overview, area III. X8100.

Figure 6. - Scanning electron micrographs of Inconel X-750 fretted against Inconel X-750. Frequency, 80 hertz; normal load, 1.47 newtons; number of cycles, 2.9×10^5; amplitude, 75×10^{-6} meter; temperature, 820^0 C (1500^0 F).

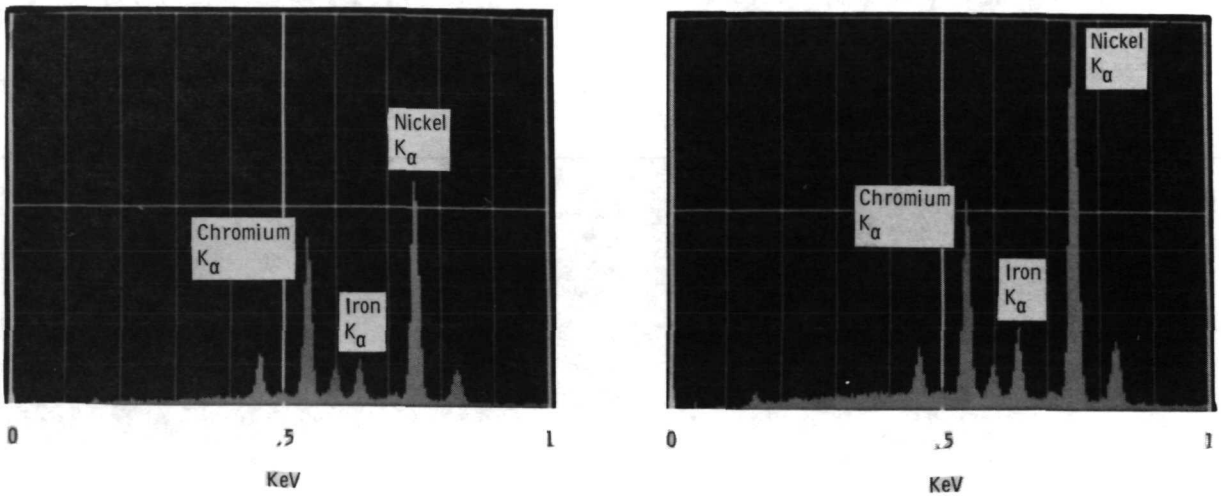

(a) Within fretting region, area corresponding to figure 6 (d).

(b) Outside fretting region.

Figure 7. - X-ray dispersion analyses of Inconel X-750 specimen surface. Temperature, 816° C (1500° F).

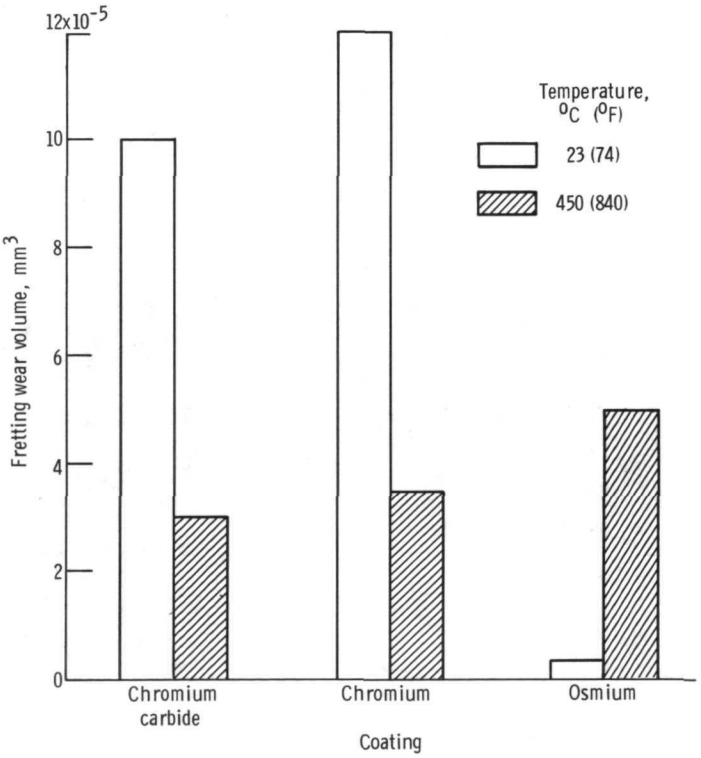

Figure 8. - Fretting wear volume on 304 stainless steel protected by various coatings. Frequency, 80 hertz; normal load, 1.47 newtons; number of cycles, $2.9x10^5$; amplitude, $75x10^{-6}$ meter.

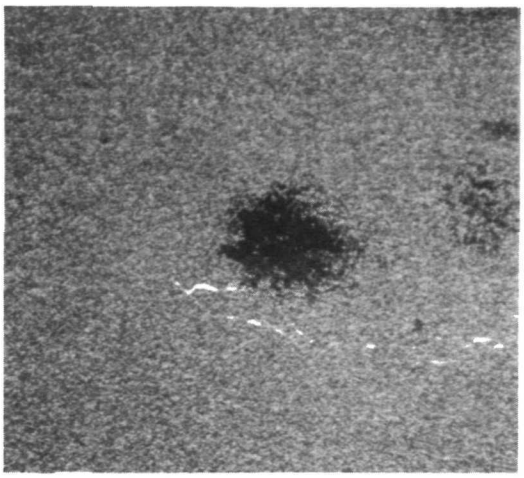

(a) Osmium at room temperature.

(b) Osmium at temperature of 450° C (840° F).

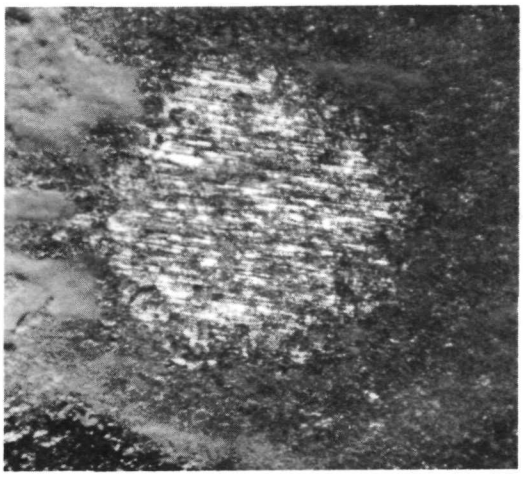

(c) Chromium carbide at room temperature.

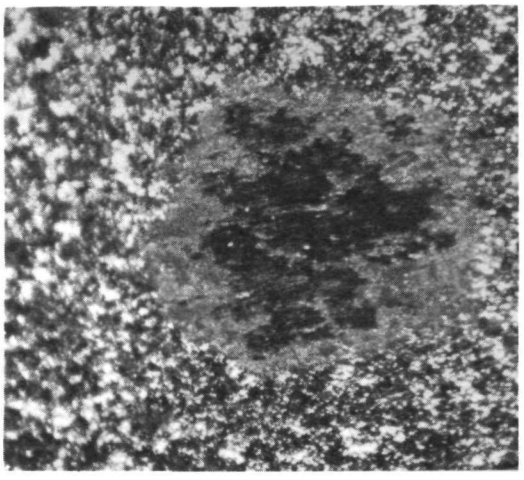

(d) Chromium carbide at temperature of 450° C (840° F).

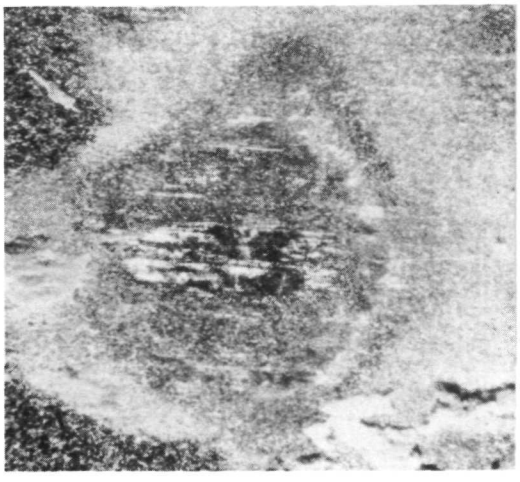

(e) Chromium at room temperature.

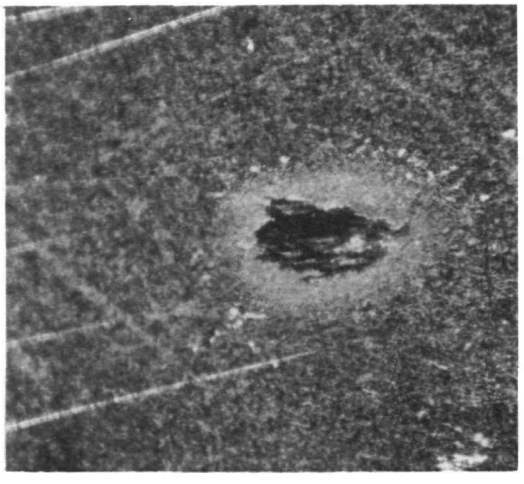

(f) Chromium at temperature of 450° C (840° F).

Figure 9. - Protective coatings on 304 stainless steel. Frequency, 80 hertz; normal load, 1.47 newtons; number of cycles, 2.9×10^5; amplitude, 15×10^{-6} meter. X75.

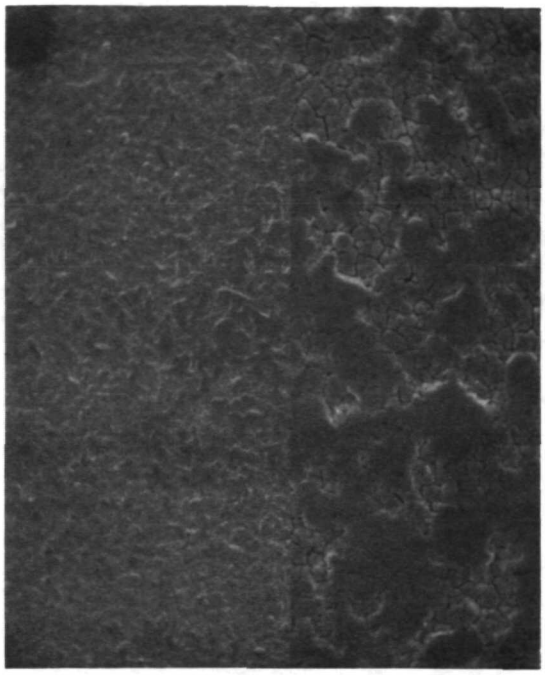

(a) Number of cycles, 10^3. X300 on left side; X900 on right side.

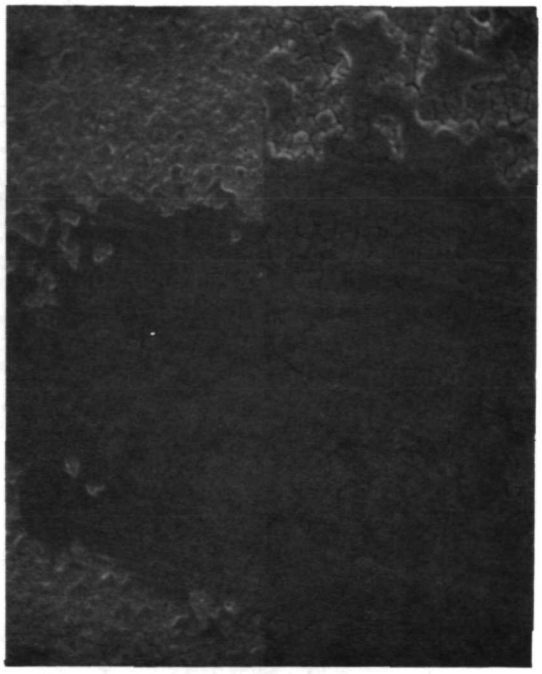

(b) Number of cycles, 10^4. X300 on left side; X900 on right side.

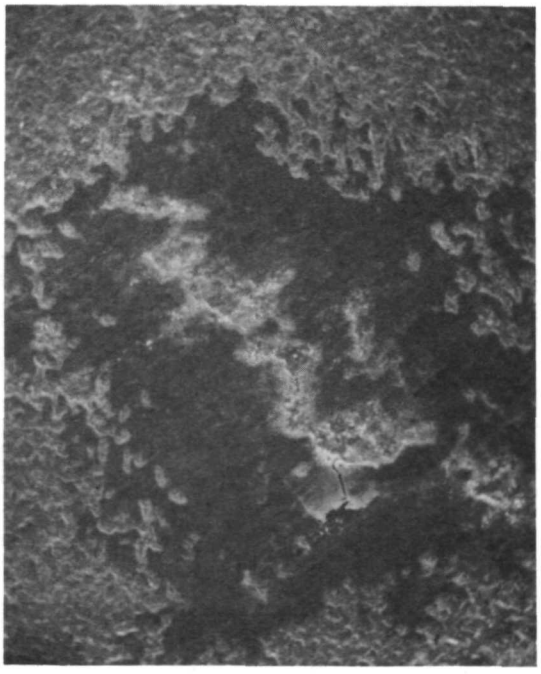

(c) Number of cycles, 2.9×10^5. X300.

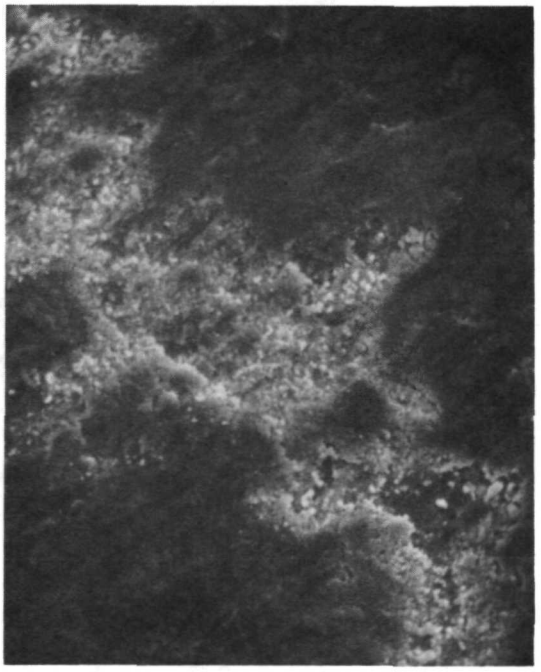

(d) Number of cycles, 2.9×10^5. X900.

Figure 10. - Scanning electron micrographs of osmium-plated 304 stainless steel fretted at room temperature. Frequency, 80 hertz; normal load, 1.47 newtons; amplitude, 75×10^{-6} meter.

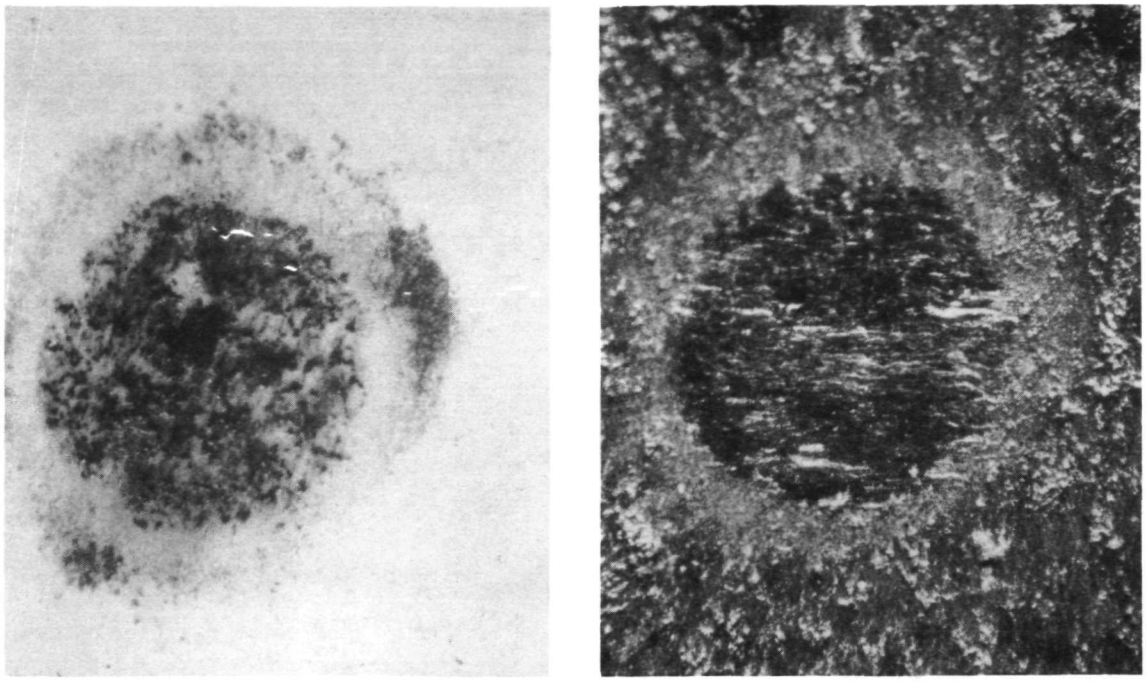

(a) Boron nitride hemisphere.

(b) High-graphite carbon flat.

Figure 12. - Boron nitride hemisphere fretted against high-graphite carbon flat. Frequency, 80 hertz; normal load, 1.47 newtons; number of cycles, 2.9×10^5; amplitude, 75×10^{-6} meter; temperature, 327° C (620° F). X75.

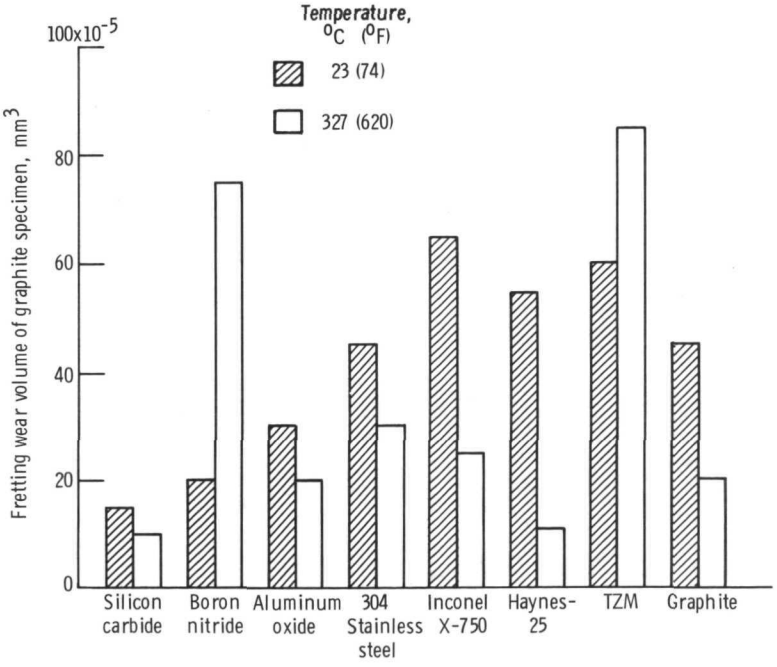

Figure 11. - Fretting wear volume of high-graphite carbon fretted against various materials. Frequency, 80 hertz; normal load, 1.47 newtons; number of cycles, 2.9×10^5; amplitude, 75×10^{-6} meter.

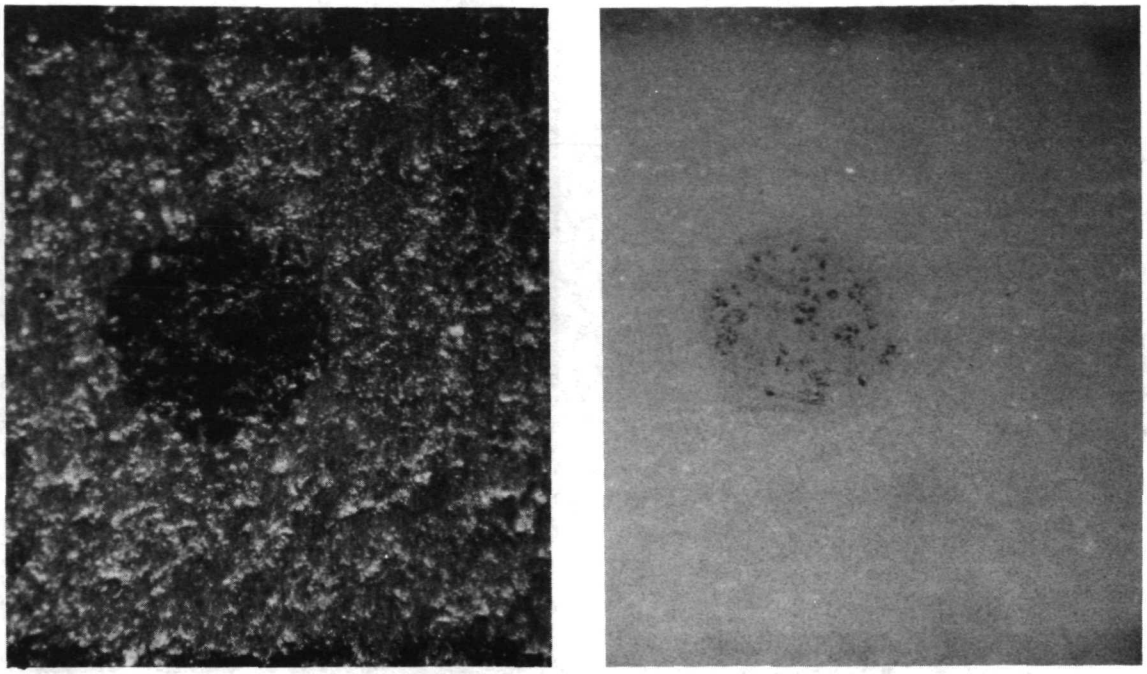

(a) Aluminum oxide hemisphere.

(b) High-graphite carbon flat.

Figure 13. - Aluminum oxide hemisphere fretted against high-graphite carbon flat. Frequency, 80 hertz; normal load, 1.47 newtons; number of cycles, 2.9×10^5; amplitude, 75×10^{-6} meter; temperature, 327^0 C (620^0 F). X75.

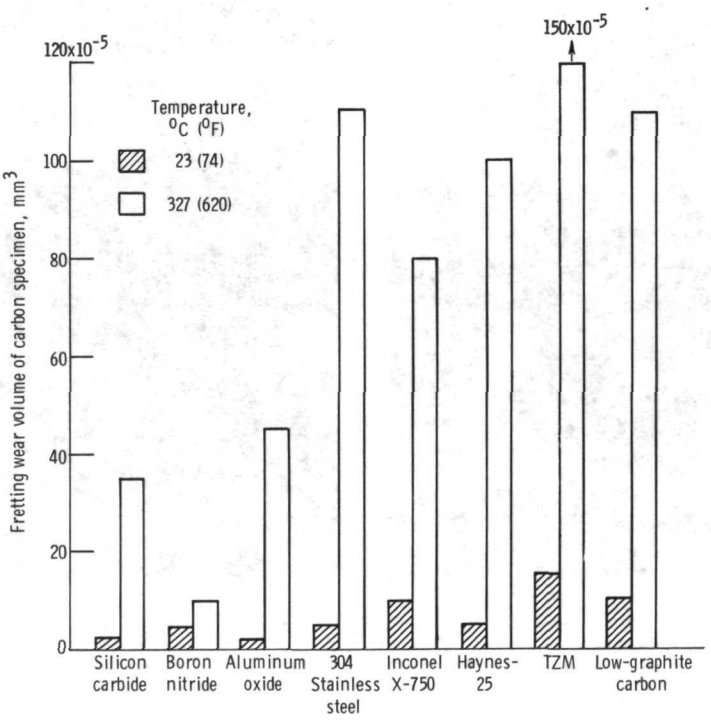

Figure 14. - Fretting wear volume of low-graphite carbon fretted against various materials. Frequency, 80 hertz; normal load, 1.47 newtons; number of cycles, 2.9×10^5; amplitude, 75×10^{-6} meter.

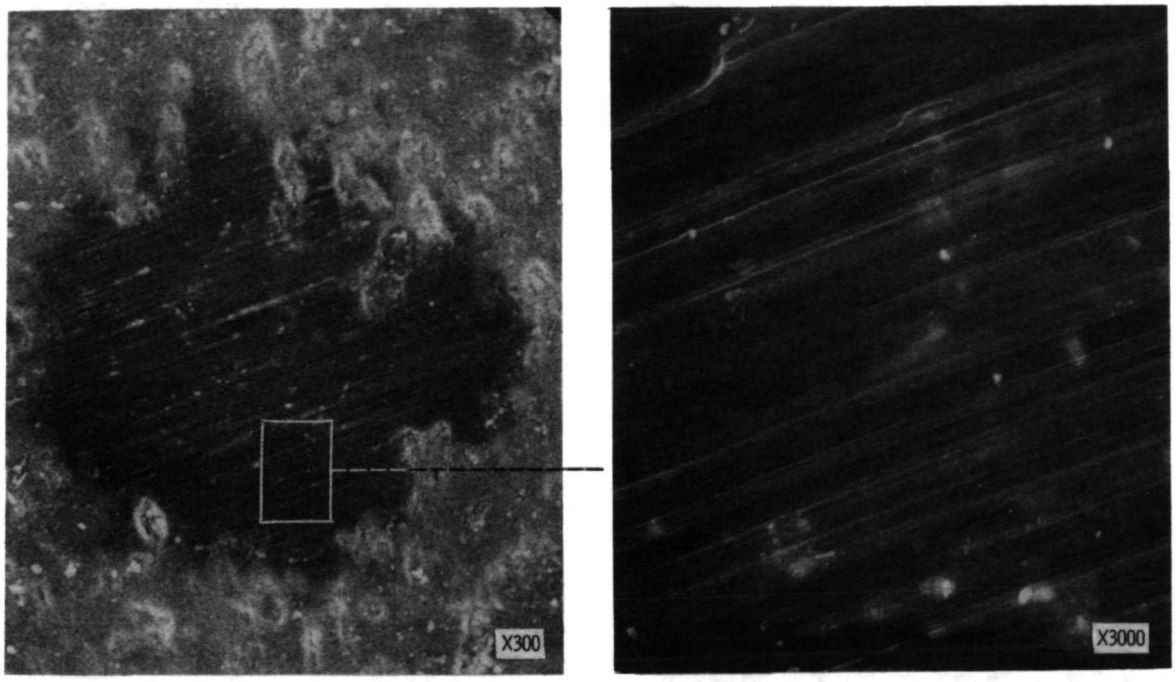

(a) Low-graphite carbon fretted against Inconel X-750.

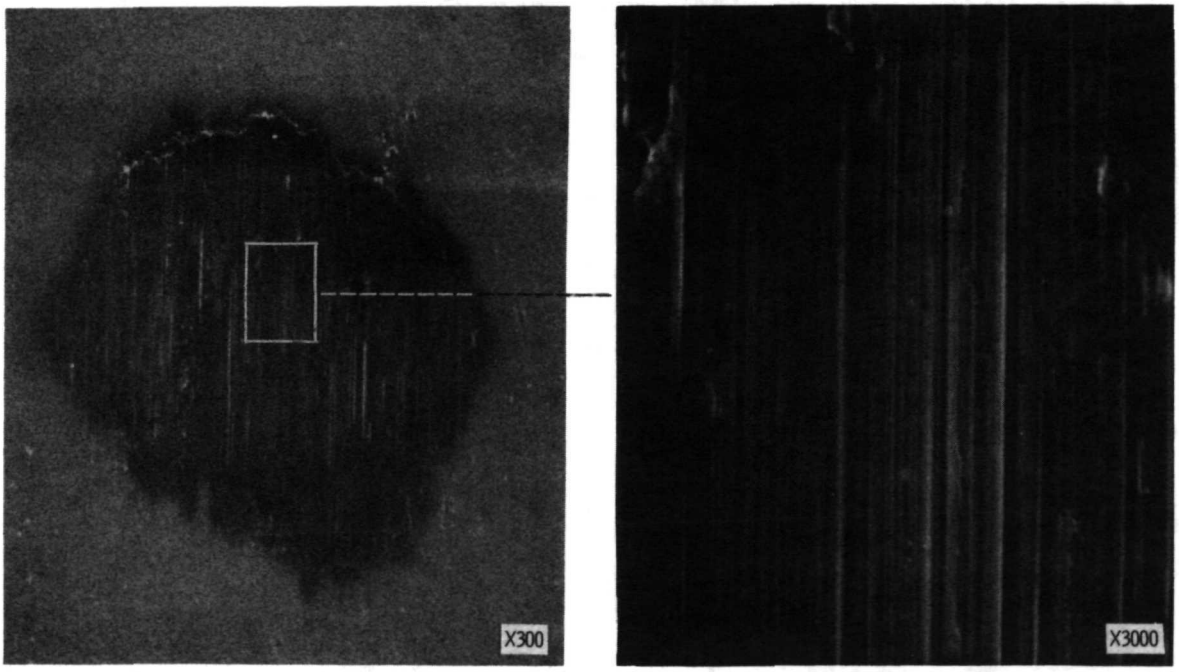

(b) Inconel X-750 sphere fretted against low-graphite carbon.

Figure 15. - Scanning electron micrographs of low-graphite carbon fretted against Inconel X-750. Frequency, 80 hertz; normal load, 1.47 newtons; amplitude, 75×10^{-6} meter; room temperature.

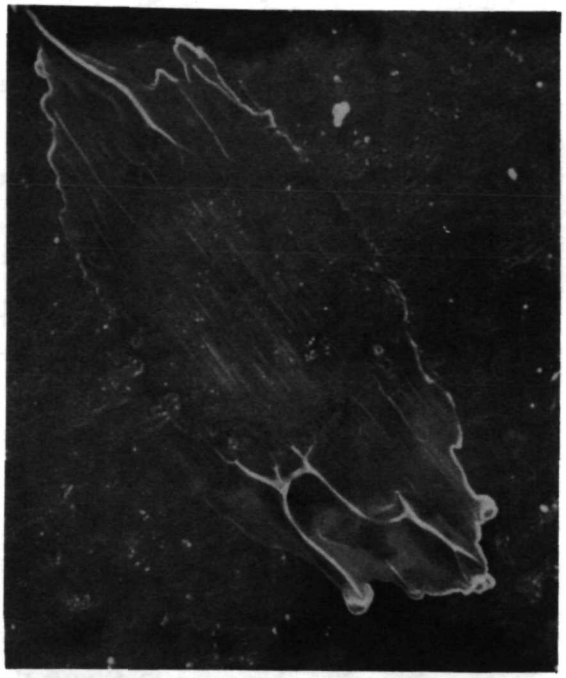

(a) Overview. X150.

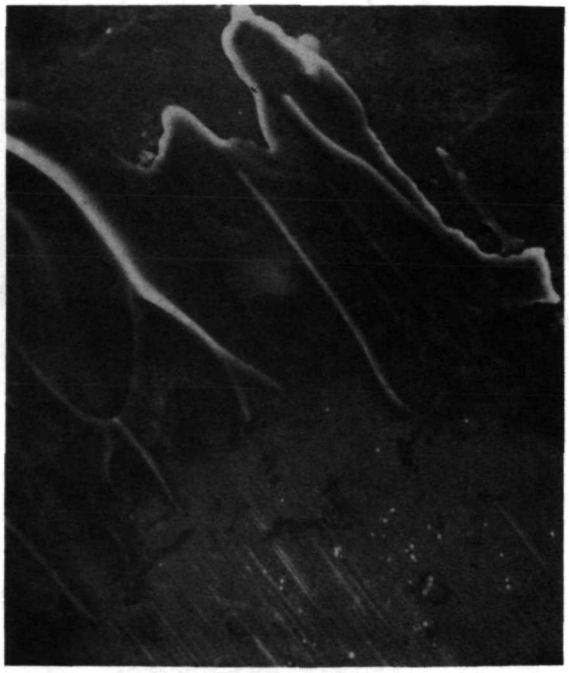

(b) Nickel deposit at ends of fretting scar. X300.

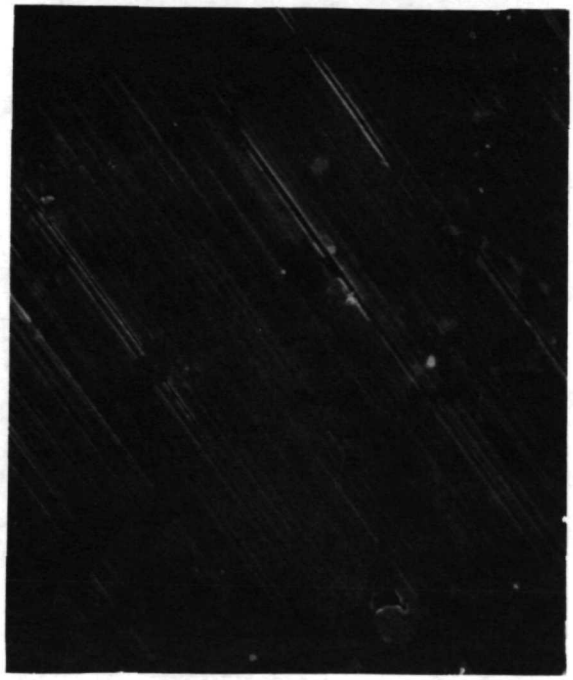

(c) Central region of fretting scar. X3000.

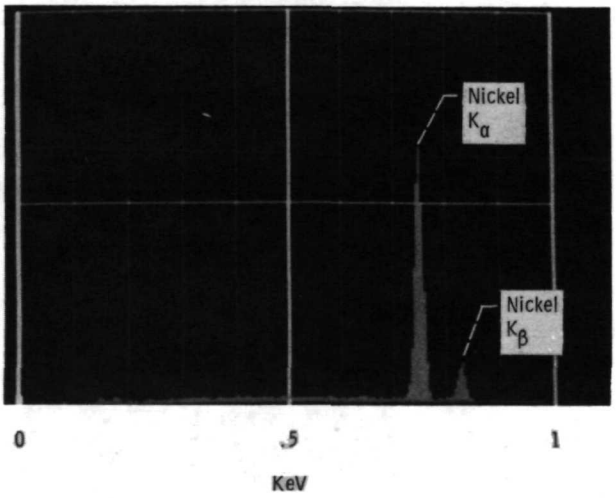

(d) X-ray dispersion analysis of deposit at end of fretting scar.

Figure 16. - High-graphite carbon fretted against 99.9 percent nickel. Frequency, 80 hertz; normal load, 1.47 newtons; number of cycles, 2.9×10^5; amplitude, 75×10^{-6} meter; room temperature.

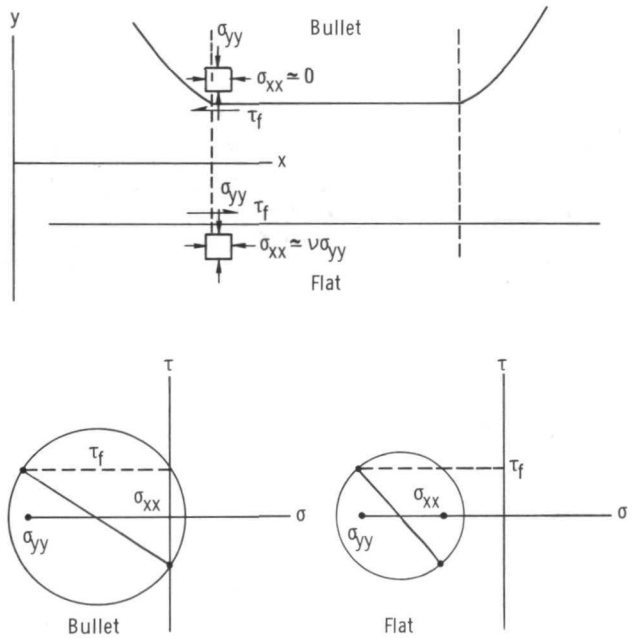

Figure 17. - Stress state at edge of contact zone on bullet (spherical tip) and on flat specimen surfaces.

(a) Edge of fretting scar showing debris particles. X300.

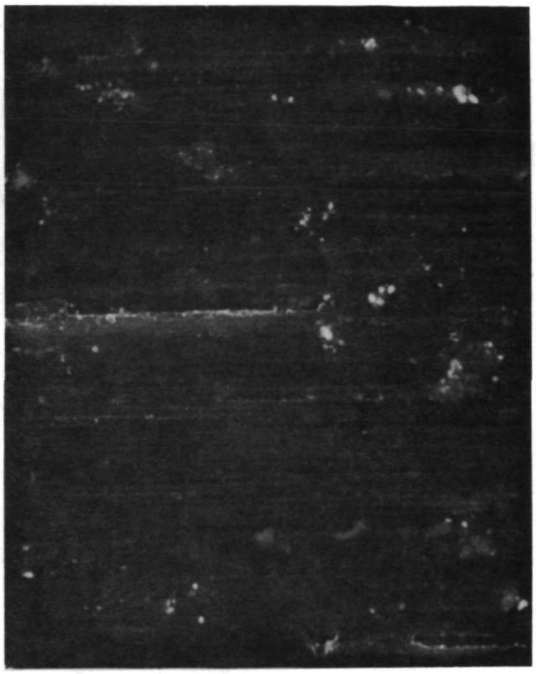

(b) Central region of fretting scar. X900.

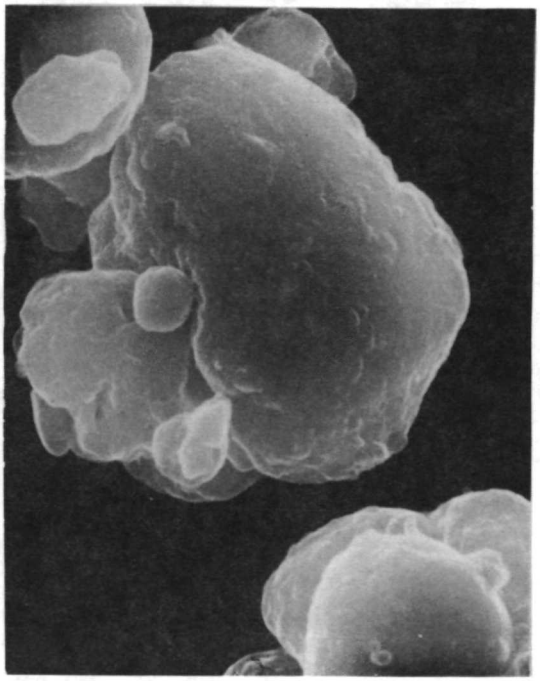

(c) Single debris particle. X12 000.

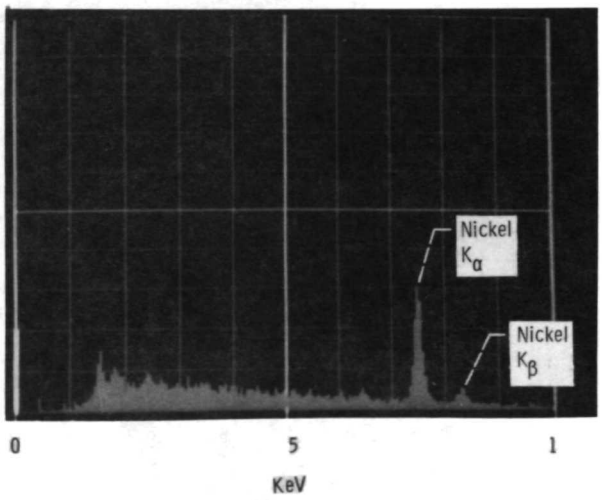

(d) X-ray dispersion analysis of debris particle.

Figure 18. - Scanning electron micrographs of low-graphite carbon fretted against 99.9 percent nickel. Frequency, 80 hertz; normal load, 1.47 newtons; number of cycles, 2.9×10^5; amplitude, 75×10^{-6} meter; room temperature.

NATIONAL AERONAUTICS AND SPACE ADMINISTRATION
WASHINGTON, D.C. 20546

OFFICIAL BUSINESS
PENALTY FOR PRIVATE USE $300

SPECIAL FOURTH-CLASS RATE
BOOK

POSTAGE AND FEES PAID
NATIONAL AERONAUTICS AND
SPACE ADMINISTRATION
451

U.S.MAIL

POSTMASTER : If Undeliverable (Section 158 Postal Manual) Do Not Return

"The aeronautical and space activities of the United States shall be conducted so as to contribute . . . to the expansion of human knowledge of phenomena in the atmosphere and space. The Administration shall provide for the widest practicable and appropriate dissemination of information concerning its activities and the results thereof."

—NATIONAL AERONAUTICS AND SPACE ACT OF 1958

NASA SCIENTIFIC AND TECHNICAL PUBLICATIONS

TECHNICAL REPORTS: Scientific and technical information considered important, complete, and a lasting contribution to existing knowledge.

TECHNICAL NOTES: Information less broad in scope but nevertheless of importance as a contribution to existing knowledge.

TECHNICAL MEMORANDUMS: Information receiving limited distribution because of preliminary data, security classification, or other reasons. Also includes conference proceedings with either limited or unlimited distribution.

CONTRACTOR REPORTS: Scientific and technical information generated under a NASA contract or grant and considered an important contribution to existing knowledge.

TECHNICAL TRANSLATIONS: Information published in a foreign language considered to merit NASA distribution in English.

SPECIAL PUBLICATIONS: Information derived from or of value to NASA activities. Publications include final reports of major projects, monographs, data compilations, handbooks, sourcebooks, and special bibliographies.

TECHNOLOGY UTILIZATION PUBLICATIONS: Information on technology used by NASA that may be of particular interest in commercial and other non-aerospace applications. Publications include Tech Briefs, Technology Utilization Reports and Technology Surveys.

Details on the availability of these publications may be obtained from:

SCIENTIFIC AND TECHNICAL INFORMATION OFFICE

NATIONAL AERONAUTICS AND SPACE ADMINISTRATION

Washington, D.C. 20546